Angular Clustering in Photometric Surveys

a new window for red-shift space distortions

Martin Crocce
Institute for Space Science (ICE)
Barcelona

Photo-Z surveys

DARK ENERGY SURVEY

Pan-STARRS

More in the future :

Euclid-imaging

LSST

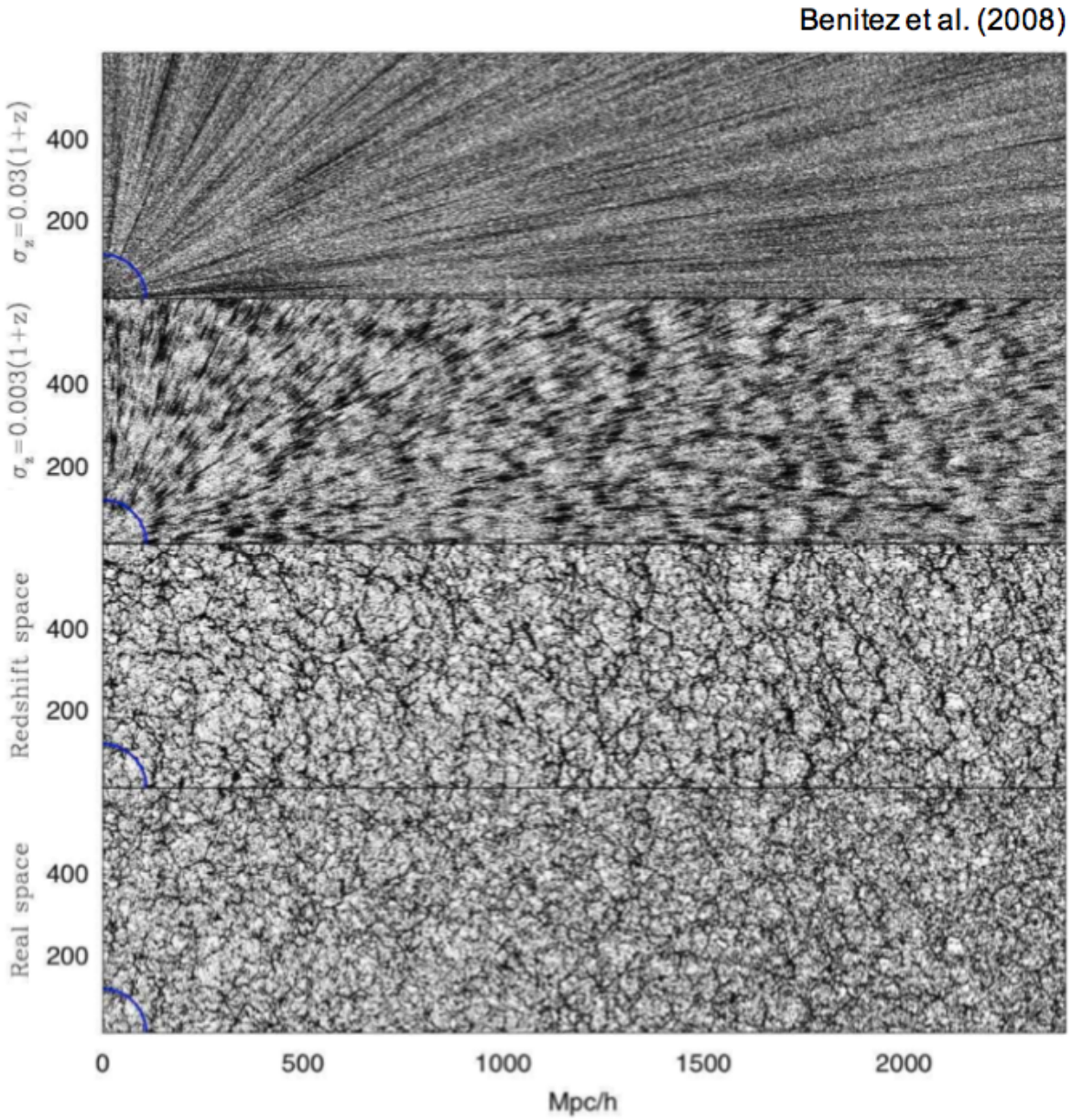

Will probe z>1 in near future. But radial positions of the galaxies will be know with quite large uncertainties (~ 100 Mpc/h), erasing the 3D-clustering information

Brief outline,

- How well can we model the clustering signal, identify most important effects. How well can we model the errors
- Theory vs. Simulated Survey Catalogs
- Forecast. What can we learn with these tools
- Proof-of-concept. Testing the tools with actual data.

Modeling the angular correlation function and its full covariance in Photometric Galaxy Surveys

Martín Crocce[1], Anna Cabré[2] & Enrique Gaztañaga[1]

[1] *Institut de Ciències de l'Espai, IEEC-CSIC, Campus UAB, Facultat de Ciències, Torre C5 par-2, Barcelona 08193, Spain*
[2] *Center for Particle Cosmology, University of Pennsylvania, 209, South 33rd Street, Philadelphia, PA, 19104, USA*

arXiv : 1004.4640

Simulations and survey mock catalogs

- Use co-moving outputs of a very large N-body simulation - MICE7680 (~ 450 cubic Gpc/*h*)
- Ensemble of mock red-shift bins, assuming 1/8 of sky and 0.2 < z < 1.4 (DES-like survey)
- Impose underlying red-shift distribution : $dN/dz \propto (z/0.5)^2 \exp\left[-(z/0.5)^{1.5}\right]$
- Include bin projection, NL clustering, bias , red-shift distortions and/or photometric errors.

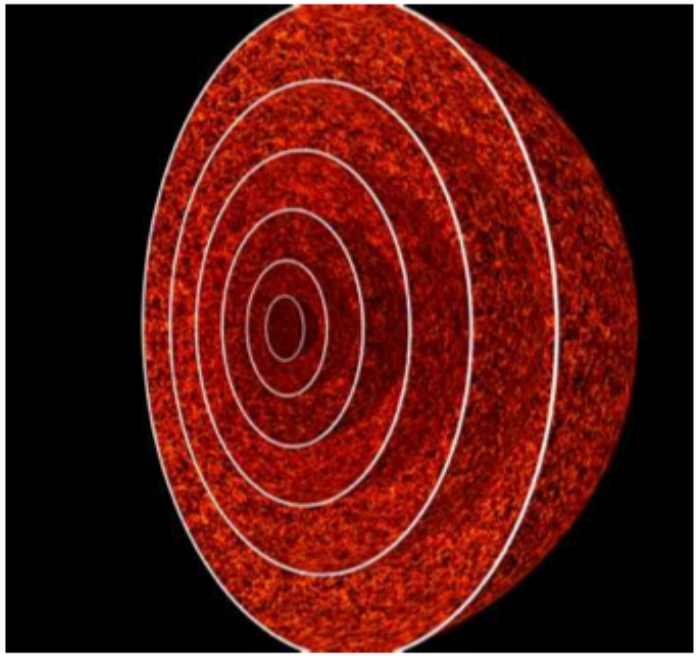

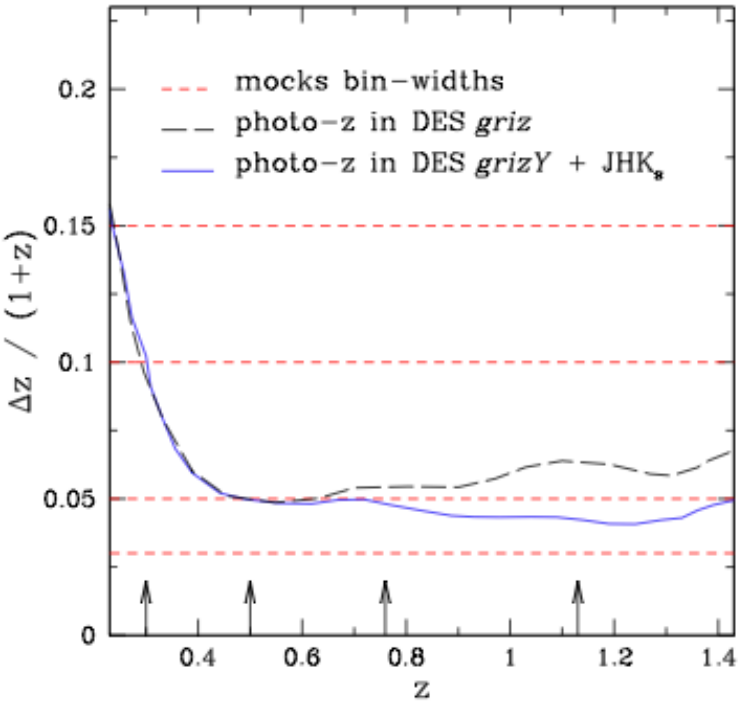

Bin widths

0.15

0.10

0.05

0.03

0.3 0.5 0.73 1.1

Bin centers

Simulations and survey mock catalogs

Real space (matter and halo field)

Real Space Mocks

$\bar{z}$	$\frac{\Delta z}{(1+z)}$	$\bar{r}$	Δr	$\bar{n}$	*Mocks*
0.3	0.03	845.7	102.65	0.11	1344
0.3	0.10	843.3	342.14	0.33	441
0.3	0.15	839.8	513.20	0.47	392
0.5	0.05	1345.8	178.23	0.48	324
0.5	0.10	1343.2	356.50	0.88	175
0.5	0.15	1338.7	534.83	1.21	150
0.73	0.05	1859.7	181.50	0.92	104
0.73	0.10	1856.5	363.10	1.68	96
0.73	0.15	1851.1	544.88	2.30	80
1.1	0.10	2558.2	360.07	2.60	36
1.1	0.15	2551.9	540.56	3.90	36

Real Space Halo Mocks

$\bar{z}$	$\frac{\Delta z}{(1+z)}$	M_{halo}	*bias*	$\bar{n}$	*Mocks*
0.3	0.15	10^{13}	2.35	$4.0\ 10^{-4}$	392
0.5	0.10	2×10^{13}	2.95	$3.2\ 10^{-4}$	175
0.5	0.10	10^{14}	4.40	$2.9\ 10^{-4}$	175

Simulations and survey mock catalogs

Red-shift and/or Photo-z space

$$\delta r = v_r(1+z)/H(z)$$

Redshift Space Mocks

$\bar{z}$	$\frac{\Delta z}{(1+z)}$	$f \equiv \frac{\partial \ln D}{\partial \ln a}$	*Mocks*
0.5	0.05	0.705	125
0.5	0.15	0.705	125

$$\sigma_r = \sigma_z c/H(z)$$

Photo-z Space Mocks

$\bar{z}$	$\frac{\Delta z}{(1+z)}$	σ_z	*Mocks*
0.5	0.05	0.06	125
0.5	0.15	0.06	125

$$f(\delta r) = \frac{1}{\sqrt{2\pi}\sigma_r} \exp\left[-\frac{\delta r^2}{2\sigma_r^2}\right]$$

Photo-z + Redshift Space Mocks

$\bar{z}$	$\frac{\Delta z}{(1+z)}$	f	σ_z	*Mocks*
0.5	0.05	0.705	0.06	125
0.5	0.15	0.705	0.06	125

@ Publicly available at *http://www.ice.cat/mice*

Modeling the angular correlation :

$$w(\theta) = \int dz_1 \Phi(z_1) \int dz_2 \Phi(z_2)\, \xi(r_{12}(\theta), \bar{z})$$

$$r_{12}(\theta) = \{r(z_1)^2 + r(z_2)^2 - 2r(z_1)r(z_2)cos(\theta)\}^{1/2}$$

Assuming linearly biased tracers and growth with respect to the mean red-shift of the bin

$$\Phi(z) = D(z, \bar{z})\, \phi(z)$$

Nonlinear Gravity and evolution

$$\begin{aligned} \xi(r,z) &= D(z)\,[\xi_{\rm Lin,0}(r) \otimes {\rm e}^{-(r/D(z)s_{bao})^2}]\,(r) \\ &+ A_{mc}\, D^4(z)\, \xi^{(1)}_{\rm Lin,0}(r)\, \xi'_{\rm Lin,0}(r) \end{aligned}$$

Use theoretical estimates for s_{bao} and A_{mc} or a fit in a single redshift b/c they scale with the growth

Red-shift Distortions :

$$\xi(r_1, r_2) = \xi(\sigma, \pi)$$

$$\xi(\sigma,\pi) = \xi_0(r_{12})P_0(\mu) + \xi_2(r_{12})P_2(\mu) + \xi_4(r_{12})P_4(\mu)$$

$$\pi = r_2 - r_1 \quad \text{and} \quad \mu = \pi/r_{12}$$

Where ξ_0, ξ_2, ξ_4 are multi-poles of ξ that depend on bias and growth rate $f \equiv \dfrac{d\ln D(a)}{d\ln a}$

Photo-z :

$$\phi(z) = \frac{dN_g}{dz} W(z).$$

$$\phi(z) = \frac{dN_g}{dz} \int dz_p P(z|z_p) W(z_p),$$

(distribution of galaxies in true red-shifts)

Modeling the error and covariance :

$$w(\theta) = \sum_{\ell \geq 0} \left(\frac{2\ell + 1}{4\pi} \right) P_\ell(cos\theta)\, C_\ell \qquad \langle a_{\ell m} a_{\ell' m'} \rangle \equiv \delta_{\ell \ell'} \delta_{m m'} C_\ell$$

$$\mathrm{Cov}_{\theta\theta'} = \sum_{\ell, \ell' \geq 0} \left(\frac{2l + 1}{4\pi} \right)^2 P_\ell(\cos\theta) P_{\ell'}(\cos\theta')\, \mathrm{Cov}_{\ell\ell'}$$

Assume that Cov ~ 1 / f_{sky} and use that in *"full sky"* $\mathrm{Var}(C_\ell) = 2\, C_\ell^2 / (2\ell + 1).$

$$\mathrm{Cov}_{\theta\theta'} = \frac{2}{f_{sky}} \sum_{\ell \geq 0} \frac{2\ell + 1}{(4\pi)^2} P_\ell(\cos\theta) P_\ell(\cos\theta')\, (C_\ell + 1/\bar{n})^2$$

$$C_{\ell,\mathrm{Exact}} = \frac{1}{2\pi^2} \int 4\pi k^2 dk P(k) \Psi_\ell^2(k) \qquad \Psi_\ell(k) = \int dz \phi(z) D(z) j_\ell(kr(z))$$

And a similar expression for red-shift space involving also $j_{\ell-2}(kr)\; j_{\ell+2}(kr)$

Angular Correlation Function : Theory vs. Mocks

Real space - Nonlinear gravity and evolution

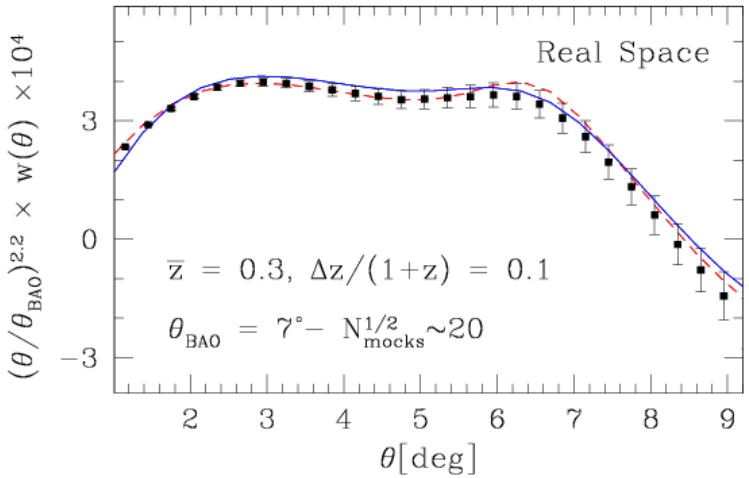

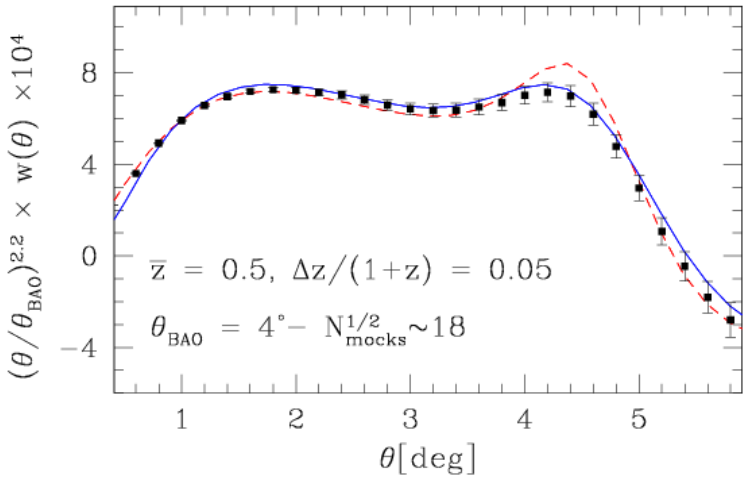

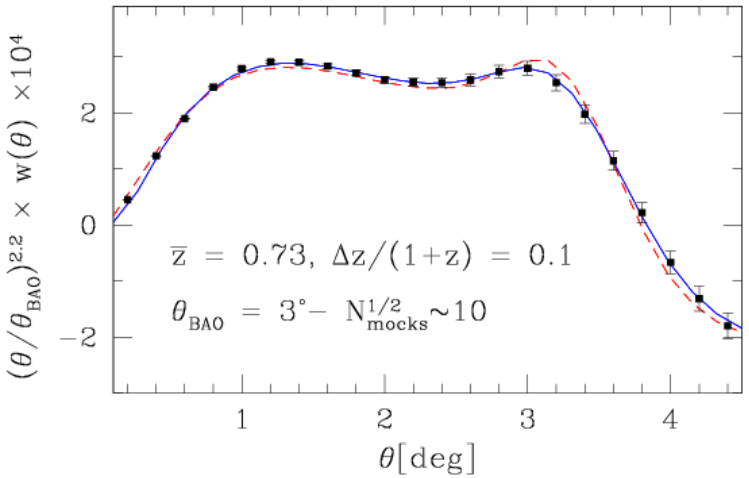

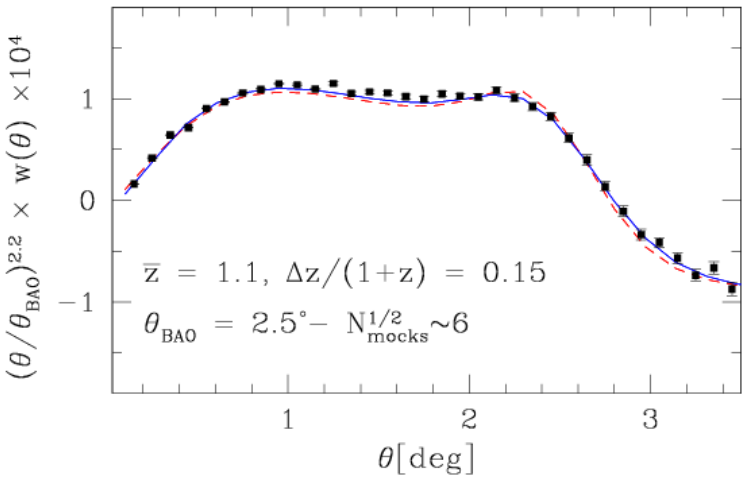

Angular Correlation Function : Theory vs. Mocks

Halo Bias

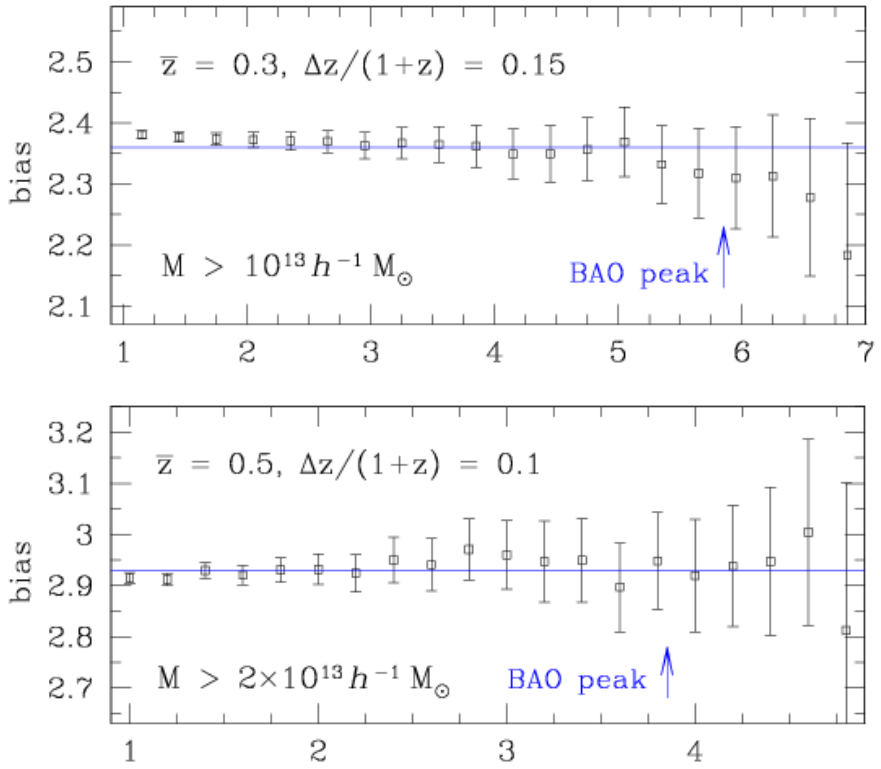

Roughly galactic halo mass scale

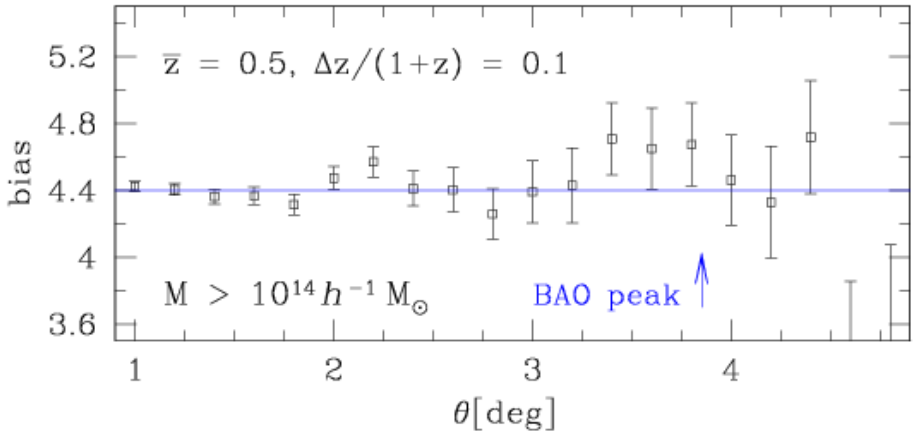

Cluster mass scale

Angular Correlation Function : Theory vs. Mocks

Red-shift Space Distortions and Photo-z effects

$$\sigma_z = 0.06 \qquad \beta = f/b = 0.7047$$

Narrow bin (width ~ 178 Mpc/h ~ photo-z)

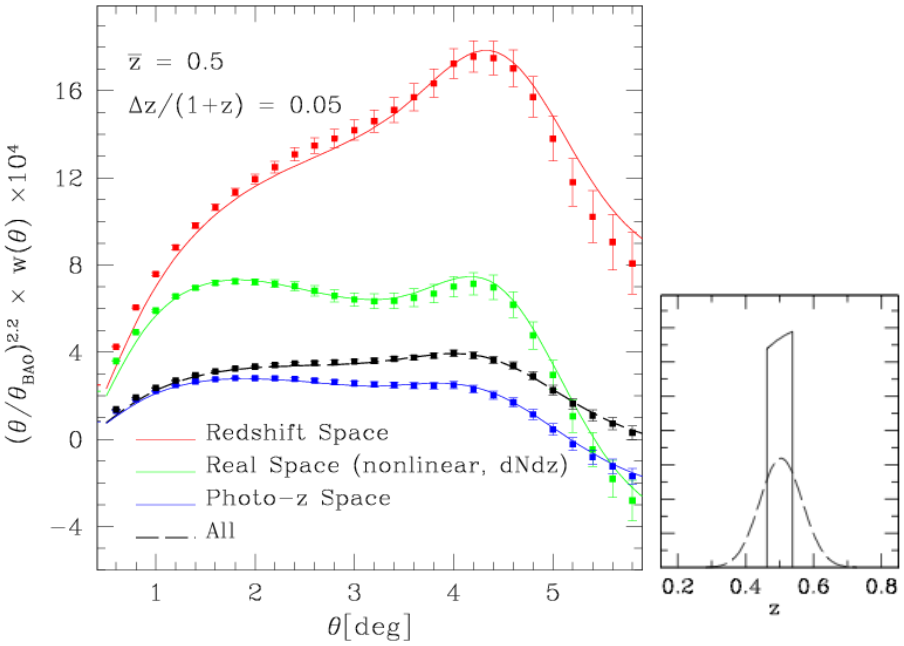

Wide bin (width ~ 500 Mpc/h ~ 4 photo-z)

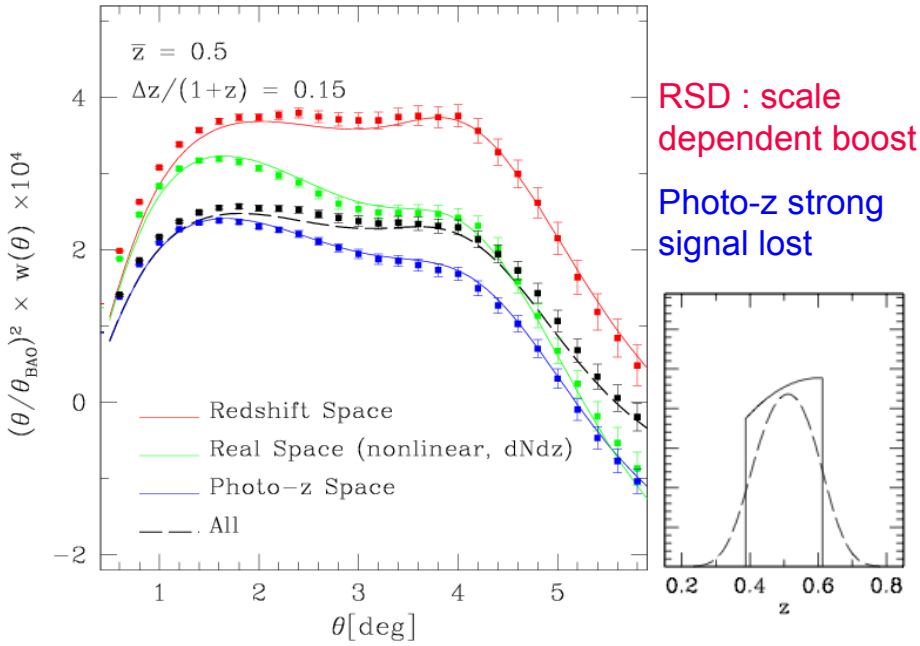

RSD : scale dependent boost

Photo-z strong signal lost

- The effect of RSD is very important even for bins as broad as 500 Mpc/h (where it “counter-acts” the photo-z smearing)
- The theoretical modeling works very nicely in all cases

Errors : Theory vs. Mocks

Red-shift and/or Photo-z space

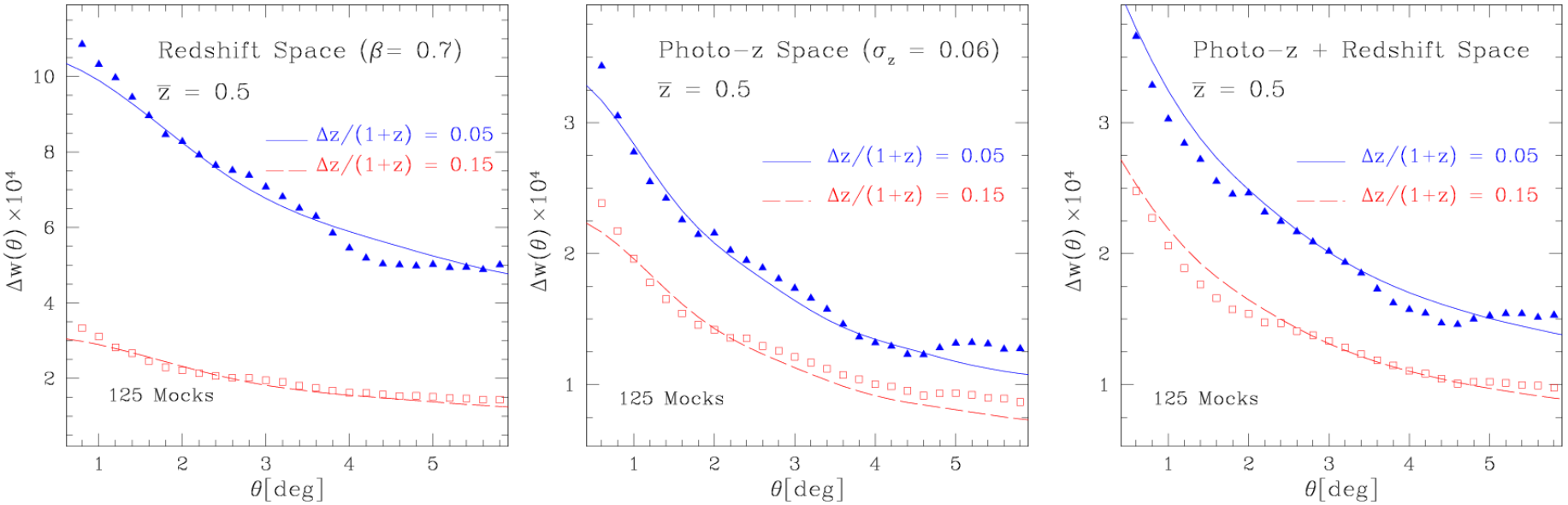

The impact of shot-noise :

Including a Poisson term 1/n into C_l

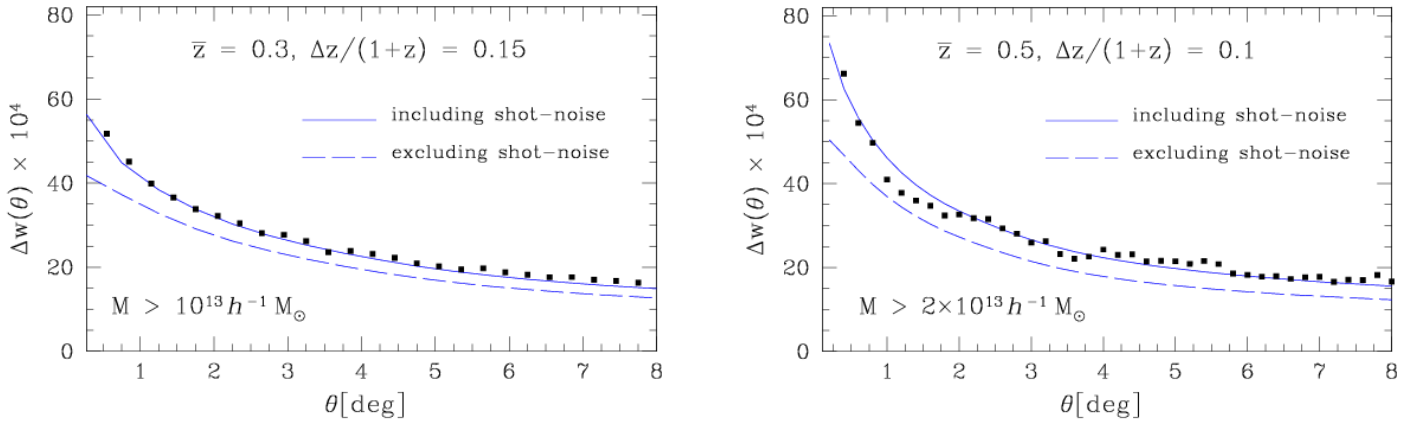

Reduced Covariance : Theory vs. Mocks

Rows of the reduced covariance

Real Space

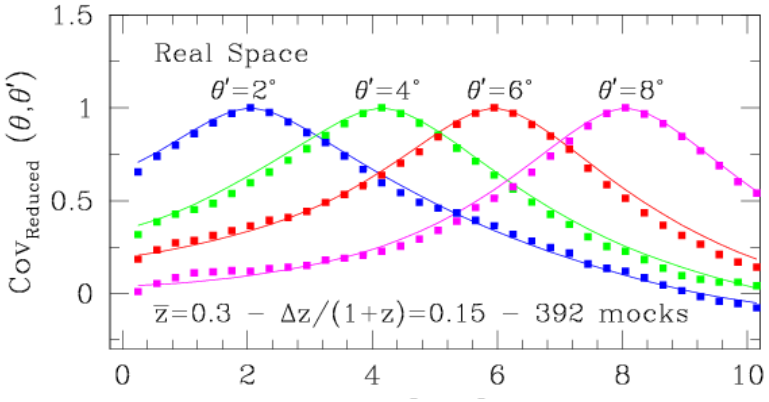

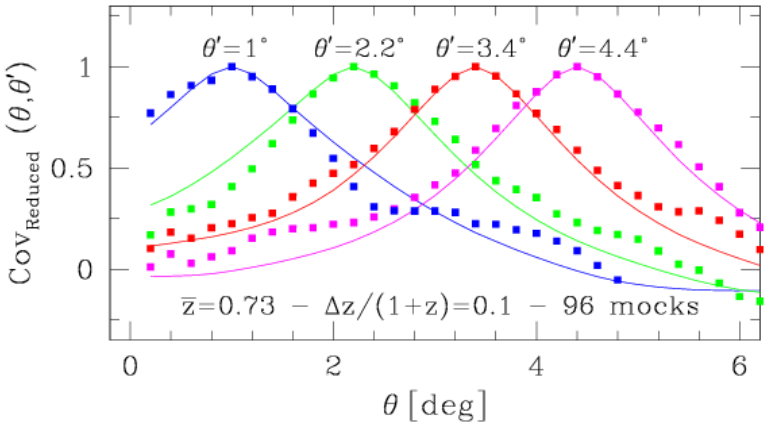

Redshift + Photo-z Space

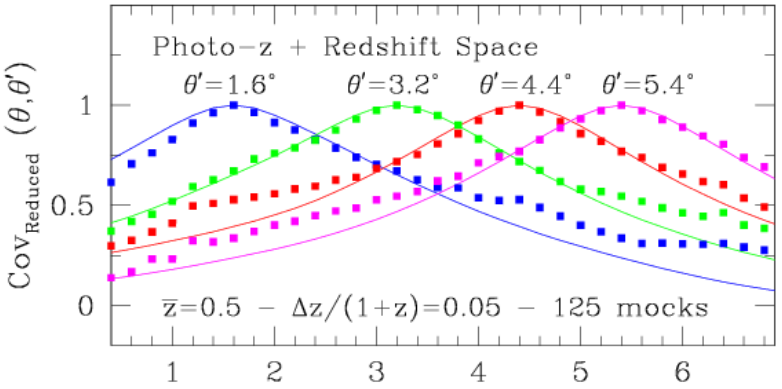

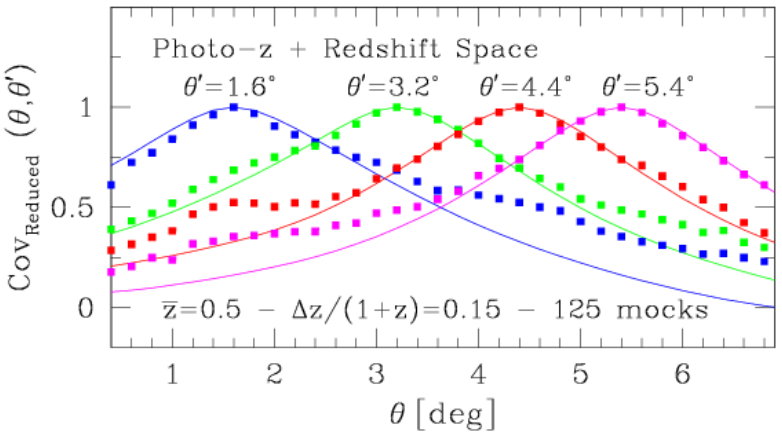

Measuring growth of structure

$$f \equiv \frac{d \ln D(a)}{d \ln a}$$

$$\xi^s(s,\mu) = \xi_0(s)P_0(\mu) + \xi_2(s)P_2(\mu) + \xi_4(s)P_4(\mu)$$

$$\xi_0(r) = (b^2 + 2bf/3 + f^2/5)\,[\xi(r)]$$
$$\xi_2(r) = (4bf/3 + 4f^2/7)\,[\xi(r) - \xi'(r)]$$
$$\xi_4(r) = (8f^2/35)\,[\xi(r) + 5/2\,\xi'(r) - 7/2\,\xi''(r)]$$

$$w(\theta) = p_0(b,f)w_0(\theta) + p_2(b,f)w_2(\theta) + p_4(b,f)w_4(\theta)$$

Collect terms in b^2, f^2 and bf

(degenerate with $\sigma_8(z)$)

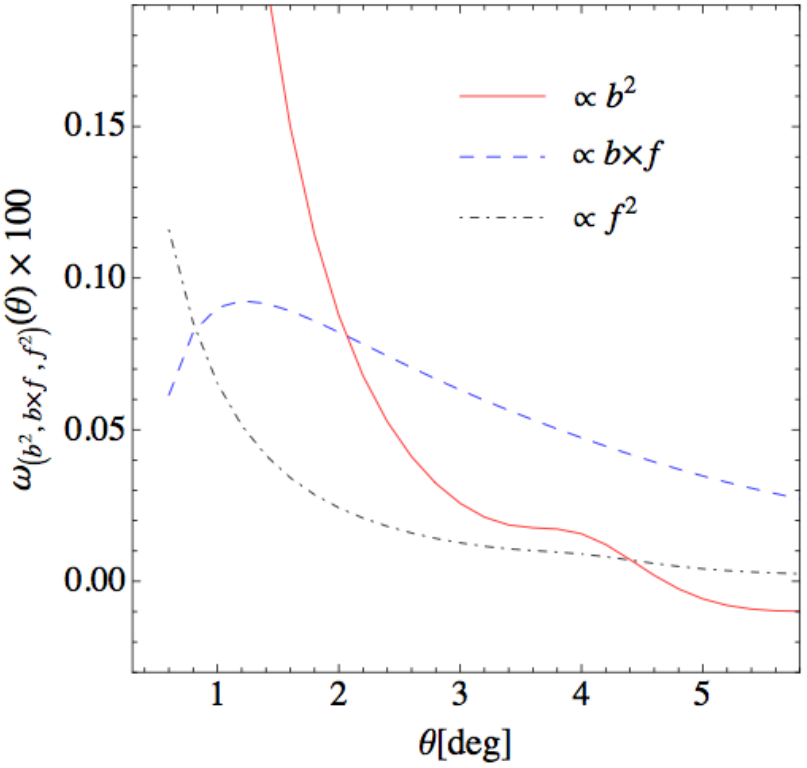

Measuring Redshift-Space Distortions using Photometric Surveys

Ashley J. Ross*[1], Will J. Percival[1], Martín Crocce[2], Anna Cabré[3], & Enrique Gaztañaga[2]
[1] *Institute of Cosmology & Gravitation, Dennis Sciama Building, University of Portsmouth, Portsmouth, PO1 3FX, UK*
[2] *Institut de Ciències de l'Espai, CSIC/IEEC, F. de Ciències, Torre C5 par-2, Barcelona 08193, Spain*
[3] *Center for Particle Cosmology, University of Pennsylvania, 209, South 33rd Street, Philadelphia, PA, 19104, USA*

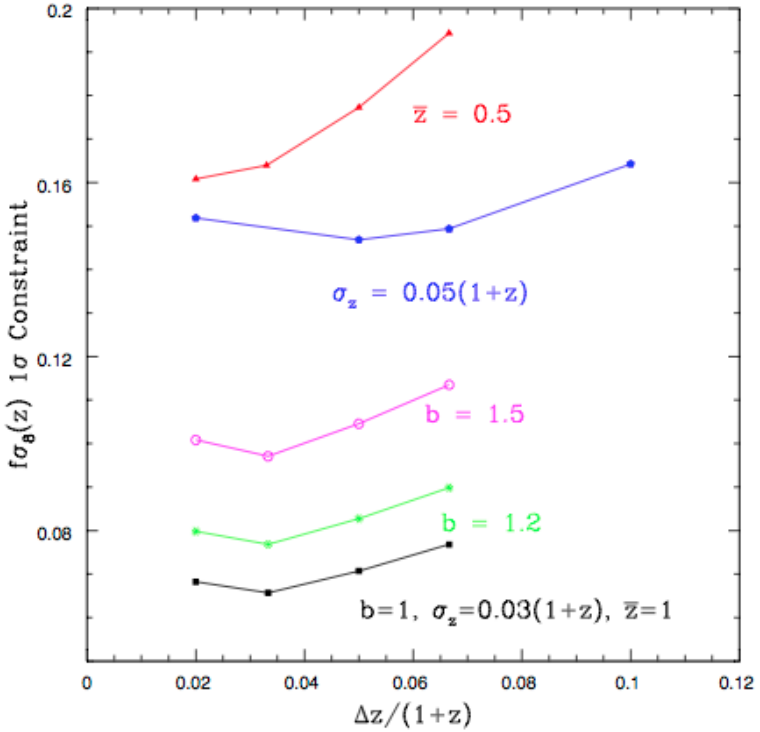

Figure 8. The black points show the expected error on $f(z)\sigma_8(z)$ versus the width of the photometric redshift bin, for unbiased tracers with average photometric redshift error $\sigma_z = 0.03(1+z)$, selected from redshift bins centred on $z = 1.065$. The other lines display the same information, for samples changed as labeled.

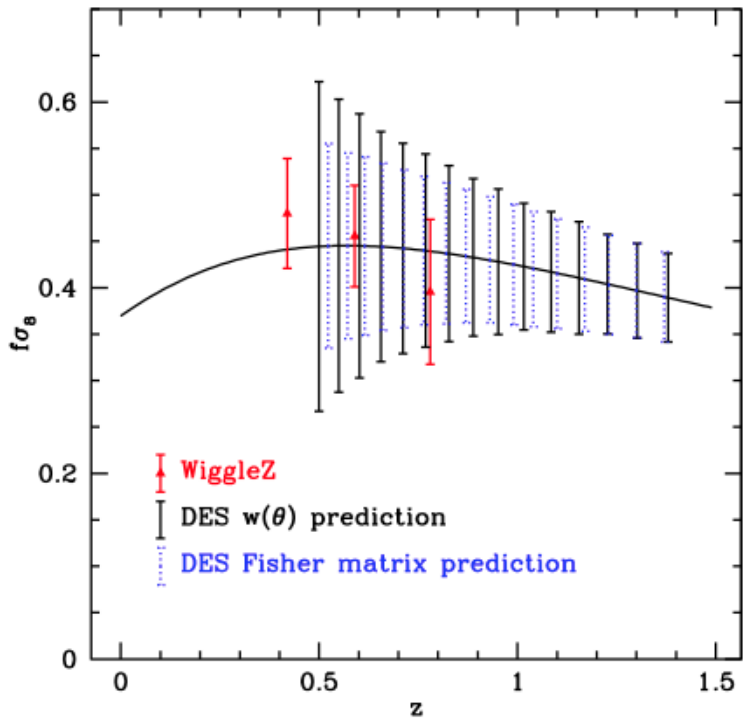

Figure 7. The solid line displays the model $f(z)\sigma_8(z)$ for our default ΛCDM model. 1σ errors (black) were calculated for the expected measurements made via successive top-hat photometric redshift bins for DES galaxies between $0.475 < z < 1.42$ and the blue error-bars display Fisher matrix predictions for similar redshift bins. The red points with 1σ errors are the measurements made with the WiggleZ survey (Blake et al. 2010).

Angular clustering in the Sloan Digital Sky Survey II

Imaging catalog of the (final) data release (DR7)

Probing the Growth of Structure and the Baryon Acoustic Feature with photometric LRGs from SDSS-DR7

M. Crocce[1⋆], A. Cabré[2], E. Gaztañaga[1], A. Carnero[3], E. Sánchez[3]
[1] *Institut de Ciències de l'Espai (IEEC-CSIC), Barcelona, Spain*
[2] *University of Pennsylvania, Philadelphia, USA*
[3] *Centro de Investigaciones Enérgeticas, Medioambientales y Tecnológicas (CIEMAT), Madrid, Spain*

- Use luminous red galaxies (LRG) sample in the imaging catalog of the final Data Release (DR7) of SDSS II
- Angular clustering analysis at the *largest angular scales and* $0.45 < z < 0.6$
- Detailed study of systematic effects (these are very important for imaging data)
- Probe to what extent red-shift space distortions and BAO can be extracted from photometric sample
- Do we match expectations? Are we dominated by systematic effects ? Is the clustering signal compatible with LCDM or anomalous?

• Selection of the galaxy sample

• color-color cuts to select high-z LRGs (Eisenstein et al 2001) :

$$(r-i) > \frac{(g-r)}{4} + 0.36,$$
$$(g-r) > -0.72\,(r-i) + 1.7,$$

• flux limit :

$$17 < petror < 21,$$
$$0 < \sigma_{petror} < 0.5,$$

• additional cuts to minimize star contamination :

$$0 < r-i < 2,$$
$$0 < g-r < 3,$$
$$22 < mag_{50} < 24.5,$$

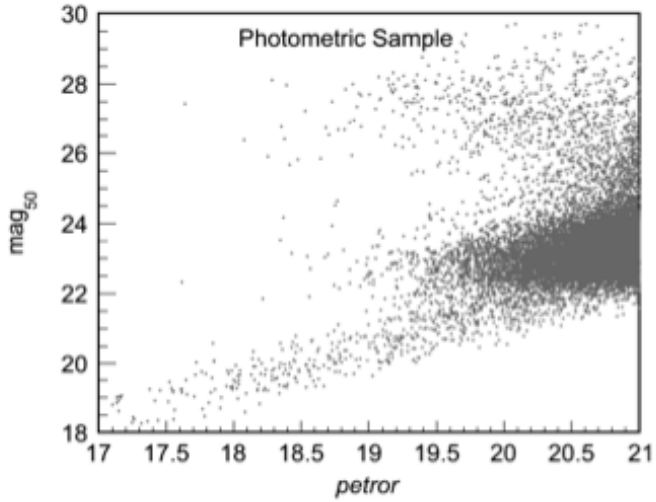

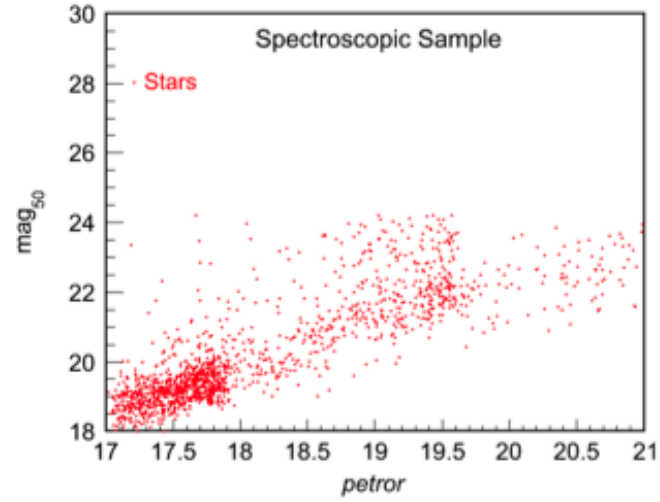

• Residual Star Contamination

• From the corresponding SDSS DR7 spectroscopic sub-sample we identify ~ 4% residual star contamination

• Using those objects identified as stars in the SDSS spec sub-sample as well as the Tychos2 star catalog we measure the angular correlation of stars,

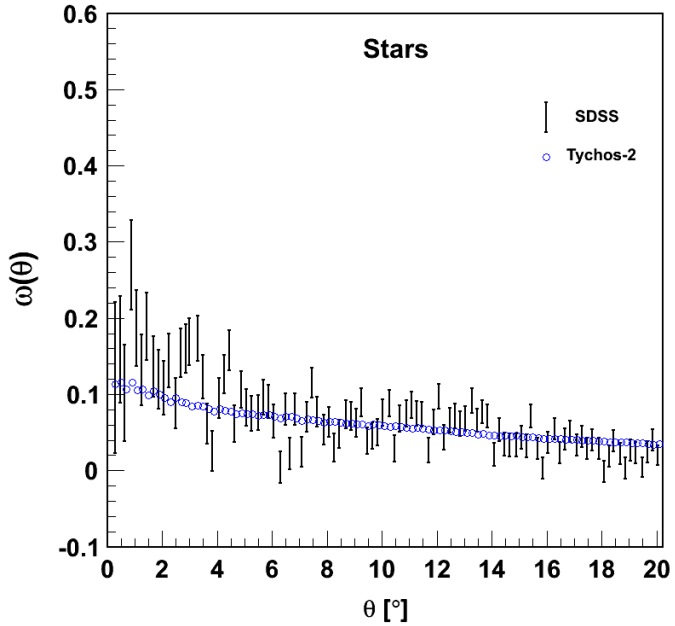

Both estimates coincide and are well fit by,

$$w_{stars,fit}(\theta) = 0.0904 - 0.00313\,\theta$$

$$w_{obs,model}(\theta, z) = (1 - f_{stars})^2 w_{gal,model}(\theta, z) + f_{stars}^2 w_{stars,fit}(\theta)$$

• Photo-z and red-shift distribution

• We used the value added catalog of Cunha et al 2009 (also Lima et al 2008) available at http://www.sdss.org/dr7/products/value_added

• It provides accurate red-shift probability distributions p(z) for each galaxy

• The true distribution of galaxies is then estimated as : $N(z) = \sum_{i=1}^{N_{gal,bin}} p_i(z).$

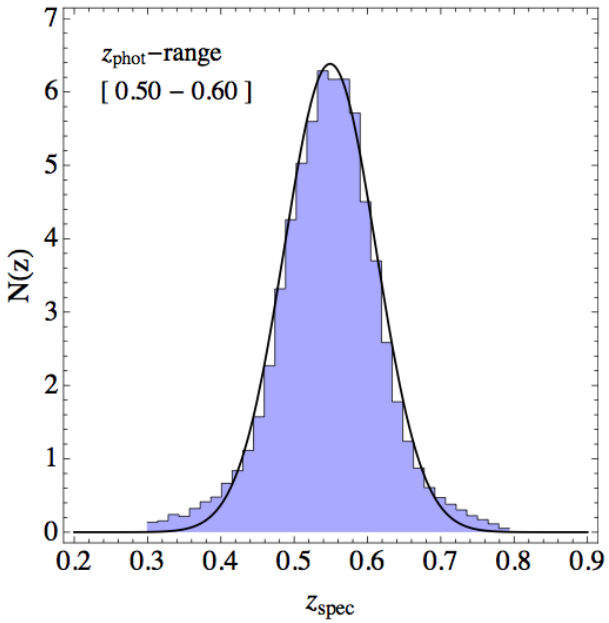

Figure 7. True (spectroscopic) redshift distribution for the bin $0.5 - 0.6$ resulting from sum of the individual redshift probability distributions. A fit to a Gaussian function (shown in solid black) yields a media of $\mu = 0.549$ and standard deviation $\sigma = 0.062$.

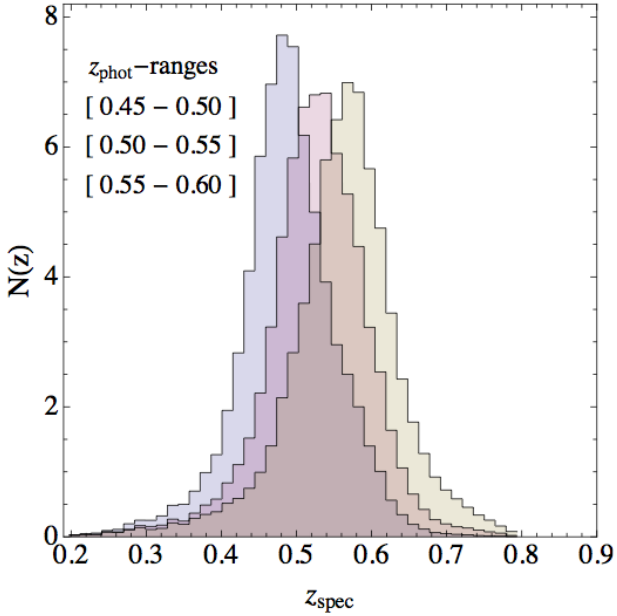

Figure 8. True redshift distribution for a set of "narrow" bins of width similar to the typical photometric error ($\Delta z = 0.05$).

- Data vs. Model I :

Red-shift Space Distortions

redshift bin	$b(z)\sigma_8(z)$	$f(z)\sigma_8(z)$
$0.50 - 0.60$	1.12 ± 0.02	0.53 ± 0.42

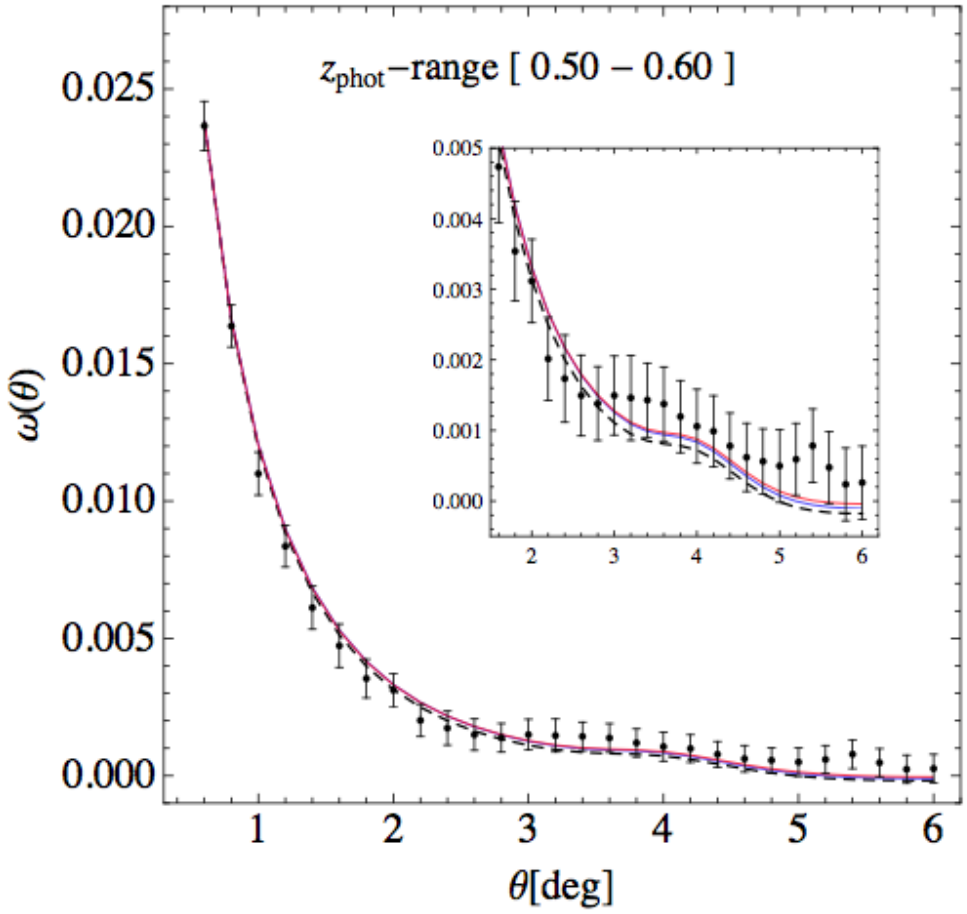

Figure 15. Angular correlation function in our central bin of width 0.1 centered at $z = 0.55$. Solid red line is our best-fit model including the effect of star contamination ($f_{star} = 4\%$). Solid blue line is the corresponding best-fit model if $f_{star} = 0$. The values for f and b are given in Table 1. For reference we include with a dashed black line a WMAP7 ΛCDM model assuming General Relativity, that is with f set to $\Omega_m^{0.55}$ ($f_{star} = 0$ in this case). The inset panel zooms in the region where the baryon acoustic peak is located (see Fig. 18 for the BAO significance). Notably the different models match the data very well in all the range of scales.

- Data vs. Model II :

  Baryon Acoustic Feature

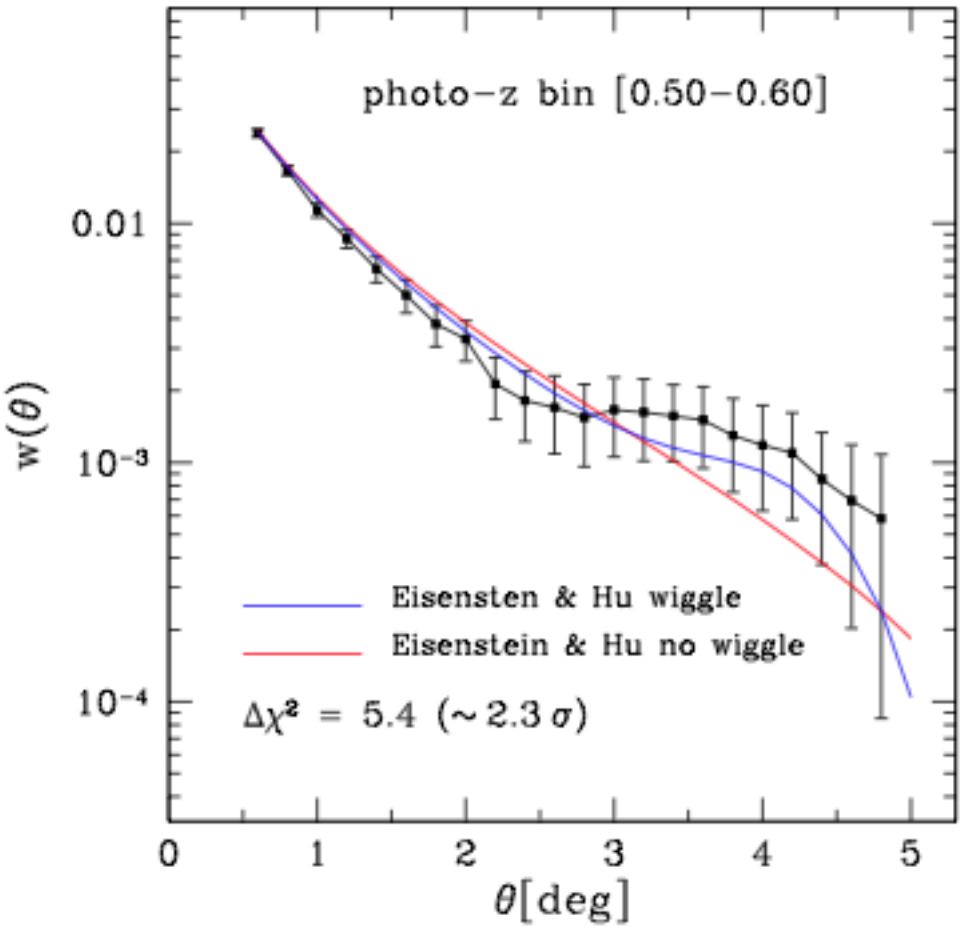

Figure 18. *Baryon Acoustic Feature at* $z = 0.55$. The plot shows the Eisenstein & Hu (1998) model with and without baryons. The data and model agree quite well in both amplitude and shape of the acoustic bump. The significance for the BAO model is $2.3\,\sigma$.

Conclusions

• Accurate and well tested model for the angular correlation function and its full covariance matrix. Good for data analysis but also for forecasts.

• Publicly available ensembles of mock catalogs from photometric surveys

• Nonlinear gravity and bias seems minor issue. Red-shift distortions is very important even for wide bins, might compete with photo-z smearing.

• A single bin at z ~ 1 in a DES-like survey should measure $f(z)\sigma_8(z)$ to $(17 \times b)\%$, comparable to current constraints from WiggleZ at z = 0.78.
Assuming several bins in 0.5 < z < 1.4 and $f(z) = \Omega_m(z)^\gamma$ should give $\gamma = 0.557^{+0.25}_{-0.22}$.

• Angular correlation function of LRGs in the imaging catalog of DR7 in good agreement with LCDM :

✓ Red-shift distortions is robustly measured matching expectations.
✓ It shows 2.3 sigma's evidence for the Baryon Acoustic Feature

Combining red-shift bins leads to stringent constrains,

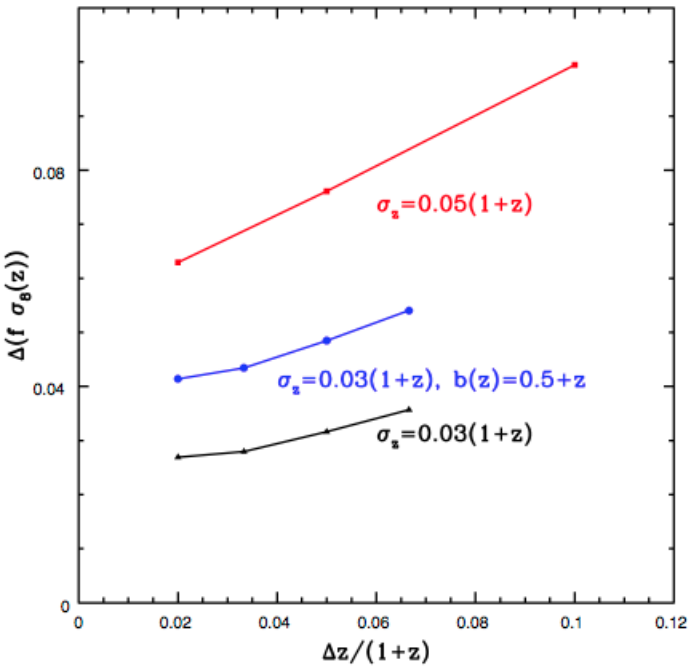

Figure 9. 68% confidence limits for a constant offset in $f(z)\sigma_8(z)$ from our fiducial model, when we combine the constraints produced by a series of $w_i(\theta)$ measured in successive redshift bins with median redshifts between 0.5 and 1.4, versus the width of the photometric redshift bins. The black symbols show the prediction for unbiased tracers with average photometric redshift error $\sigma_z = 0.03(1+z)$. The red points display the same information for $\sigma_z = 0.05(1+z)$ and the blue points assume that the bias of the selectable galaxies evolves, such that $b(z) = 0.5+z$ and the average photometric redshift error of these galaxies is $\sigma_z = 0.03(1+z)$.

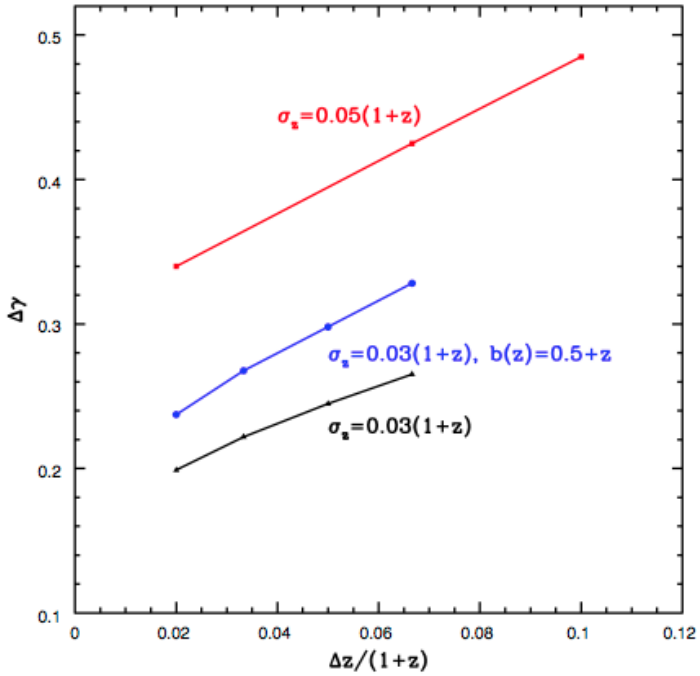

Figure 10. As Fig. 9, but now showing the expected constraints on the value of γ, given the model $f(z) = \Omega_m(z)^\gamma$.